Electronic excitation in transmission of relativistic H^- ions through thin foils

ORNL/CP-98338

C.O. Reinhold, P. Kürpick, J. Burgdörfer* , S. Yoshida,

Physics Division, Oak Ridge National Laboratory, Oak Ridge, Tennessee, 37831-6373

Department of Physics, University of Tennessee, Knoxville, Tennessee, 37996-1200

CONF-980564--

B. Gervais

Centre Interdisciplinaire de Recherche avec les Ions Lourds, Laboratoire Mixte CEA-CNRS, rue C. Bloch, Boîte Postale 5133, 14040 Caen Cedex 05, France

(May 7, 1998)

Abstract

We describe a theoretical model to study the transmission of relativistic H^- ions through thin carbon foils. Our approach is based on a Monte Carlo solution of the Langevin equation describing electronic excitations of the atoms during the transport through the foil. Calculations for the subshell populations of outgoing hydrogen atoms are found to be in good agreement with recent experimental data on an absolute scale and show that there exists a propensity for populating extreme Stark states.

PACS: 34.50.Fa, 34.10.+x

---

*Present address: Institute for Theoretical Physics, Vienna University of Technology, A-1040 Vienna, Austria

DISCLAIMER

I. INTRODUCTION

The reference design of next-generation spallation neutron sources (SNSs) features an H^- beam in the form of macropulses accelerated to $\sim$ 1 GeV in a linear accelerator (LINAC), which is stripped to bare protons by transmission through a thin foil and injected into and stored in an accumulator ring [1,2]. Filling the ring leads to compression of the pulse which after a few hundred revolutions is dumped into the spallation target. The effective conversion of H^- to H^+ and the underlying beam-foil interaction at the point of injection is a crucial element for the design of high-intensity SNSs. Since the thickness of the foil should be as small as possible to avoid excessive degradation of the beam by angular straggling, stripping to H^+ is incomplete and results in a fraction of outgoing H^0 atoms. Neutral hydrogen exits the foil in excited states which then get stripped by the strong magnetic field in the first bending magnet. The resulting protons collide with walls and magnets leading to high levels of radioactivity along the beam line. For envisioned high intensity SNSs in the 1MW range, suppression of this activation is essential and any strategy to control it requires a detailed study of the excited-state distribution of the neutral fraction.

We have recently started a research effort directed towards developing realistic classical and quantum mechanical transport simulations for the conditions that are encountered in current designs of SNSs [3,4]. A complementary experimental effort has been pursued at the Los Alamos meson factory (LAMPF) [5–7]. These include investigating effects on the stripping process due to relativistic excitations and magnetic fields as well as the relative subshell populations of excited states of hydrogen upon foil exit. In this work we briefly describe our approach and we present some recent results. Atomic units are used throughout.

II. THEORY

The theoretical method used in the present paper has been extensively described elsewhere [8,3,4]. We therefore restrict ourselves to a brief summary. Our transport theory

reduces the complex problem of H^-(1s,1s')-solid interaction to two major steps. First, the weakly bound "outer" 1s' electron is collisionally detached. Secondly, the resulting H atom propagates through the solid experiencing multiple collisions.

The probability for destruction of H^- as a function of the foil thickness x is given by $P_{H^-}(x) = e^{-x/\lambda_D}$, where the inverse mean free path (IMFP) for collisional single-electron detachment of H^-, λ_D^{-1}, is approximately given by the total IMFP of free electrons [3]. The sudden collisional removal of the outermost electron leads to a redistribution (shake-up) of the inner electron of H^- among hydrogenic states. Using the generalized shake-up approximation and the 20-parameter H^- wavefunction of Hart and Herzberg [9], it is found that predominantly H(1s) and H(2s) become populated [3] (about 90% in the 1s state). The probability for destruction of H^- and the probabilities for shake-up into individual hydrogenic states provide the source strength per unit path length for populating a given H(ns) state entering the transport simulation.

Having generated an initial H(ns) state after collisional detachment and shake-up, the evolution of the hydrogenic electron in the rest frame of the proton is governed by a non-relativistic Hamiltonian

$$\mathcal{H}(t) = \mathcal{H}_{at} - \vec{r}\cdot\vec{F}_c(t) = \frac{p^2}{2} - \frac{1}{r} - \vec{r}\cdot\vec{F}_c(t), \tag{2.1}$$

where $\vec{r}$ and $\vec{p}$ are the position and momentum vectors of the electron and $\mathcal{H}_{at}$ is the atomic Hamiltonian. The energy and angular straggling of the proton are very small and have a negligible effect on the dynamics of the electron. Thus, the proton is assumed to move on a straight line at constant relativistic velocity, v_p' (we use primes to denote laboratory frame variables).

The Newton equation associated with the Hamiltonian in Eq. 2.1 has the form of a stochastic Langevin equation. The stochastic force $\vec{F}_c(t)$ represents the interaction of the electron with the solid and is given by a sequence of impulsive momentum transfers ("kicks")

$$\vec{F}_c(t) = \sum_\alpha \sum_i \Delta\vec{p}_i^{\,\alpha}\delta(t - t_i^\alpha) \tag{2.2}$$

where α denotes the different types of elastic and inelastic collisions suffered by the electron. Elastic collisions represent elastic scattering of the electron at the screened heavy nuclei in the solid. Inelastic collisions consist of single-particle-single-hole and collective excitations of electrons in the foil. Both the destruction of H^- and the excitation and ionization of H in subsequent elastic and inelastic collisions are evaluated in linear response theory, or equivalently, in the Born approximation for a quasi-free electron propagating at relativistic velocities through the solid. However, all collisions take place in the Coulomb field of the projectile and, therefore, we treat the time evolution non-perturbatively.

The probability distributions of impulsive momentum transfers and flight times, $(\vec{p}_i^{\alpha}, \Delta t_i^{\alpha})$, between "kicks" are determined from the relativistic differential inverse mean free paths (DIMFPs) for free electrons [3]. Elastic momentum transfers are calculated from the differential elastic cross section for the scattering of electrons at the target cores. Inelastic momentum transfers are obtained from a realistic dielectric function of the foil as a function of the frequency and wavevector [10]. We consider both longitudinal (non-relativistic) and transverse (relativistic) excitations [11,12]. Figure 1 shows the mean free paths associated with the different collisional processes. While stopping powers increase with energy in the relativistic regime, the mean free paths saturate at large energies. This is due to the fact IMFPs are the zeroth moment $< E^0 >$ of the energy transfer whereas the stopping power is the first moment $< E^1 >$, which places a larger weight on large energy transfers. Since population fractions are more directly related to the IMFPs rather than to the average energy transfers, the saturation of the MFPs implies a similar result for the population fractions of the transmitted beam. The main relativistic effect in our calculations is associated with transverse electromagnetic excitations. The mean free path for these excitations decreases for increasing velocity and this process becomes increasingly important. For carbon foils, however, Fig.1 indicates that collisional processes are dominated by longitudinal excitations and elastic scattering. Inelastic longitudinal collisions have the shortest mean free path while elastic collisions have the largest momentum transfers among the scattering processes.

III. CLASSICAL TRANSPORT

The time evolution of the electronic state of the hydrogen atom can be studied using a classical trajectory approach. Within this approximation, the quantum wavefunction is replaced by a classical probability density in phase space, $f(\vec{r},\vec{p},t)$ which initially mimics the quantum state after shakeup. Formally, the time evolution of this density is governed by the classical Liouville equation for the Hamiltonian $\mathcal{H}(t)$ in Eq. 2.1. Since classical phase space points evolve in time independently according to Hamilton's equations, the Liouville equation can be easily solved using a Monte Carlo technique. The resulting method is usually referred to as the classical trajectory Monte Carlo (CTMC) approach [13].

The fraction of hydrogen atoms exiting the foil is directly given by the fraction of electron trajectories for which the electron has a negative binding energy with respect to the proton. The final substate distribution of outgoing atoms are obtained from the final distribution of classical actions which are directly related to the quantum numbers. For example, the parabolic quantum numbers n,k,m (principal, Stark, and magnetic) are associated with the actions $n_c = 1/\sqrt{-2\mathcal{H}_{at}}$, $k_c = n_c * A_z$, and $m_c = L_z$ (see e.g. [14]), where $\vec{L} = \vec{r}\times\vec{p}$ is the angular momentum and $\vec{A} = \vec{p}\times\vec{L} - \hat{r}$ is the Runge-Lenz vector. The continuous distribution of final actions after exiting the foil can be mapped onto quantum states by binning these classical actions around their corresponding quantum numbers (see e.g. [15]).

Figure 2 illustrates the behavior of calculated charge state and population fractions of n-shells of hydrogen as a function of the foil thickness. For a beam energy of 800 MeV the calculations are in good agreement with experimental data of Gulley et al [6] on an absolute scale. The figure shows that the foil thickness at which the populations of $H(n=1,2)$ maximize is very different from the ones for $H(n\geq 3)$, indicating the existence of different production mechanisms. While shake-up plays a very important role in the population of the $n=1,2$ shells, $n\geq 3$ shells are predominantly populated through multiple collisions. An average of eight collisions are involved for the largest foil thickness in the figure. The present calculations are slightly different from previous ones [3] which were fortuitously

in better agreement with experiment. The reason for this discrepancy is that our previous random momentum transfer sampler was overestimating the fraction of large energy transfers delivered to the electron.

The time-dependent subshell populations of excited hydrogenic states generated during propagation of the hydrogen atom through the foil probe the relative contributions of elastic and inelastic momentum transfer as well as their absolute values and direction and allow to the identification of propensity rules favoring certain values of the quantum numbers. Recently, Keating et al. [7] have experimentally determined the subshell distributions of hydrogen atoms resulting from the transmission of 800 MeV H^- ions through foils of various thicknesses. The subshell distributions were determined using an additional downstream transverse magnetic field $\vec{B}'$. The direction of the corresponding motional electric field $\vec{E} = \gamma'_p\,(\vec{v'_p}/c) \times \vec{B}'_{lab}$ (where $\gamma'_p = 1/\sqrt{1-(v'_p/c)^2}$) is perpendicular to the beam axis and defines the quantization axis used in the following to classify the states.

Fig. 3(a) displays a comparison between our calculations and the measurements of Keating et al [7] for the outgoing m-distributions (summed over k) in the $n = 4$ shell. The agreement between theory and experiment is very good and both reveal that the $m = 0$ population is drastically enhanced compared to a statistical distribution (the statistical weight of $m = 0, 1, 2, 3$ is 0.25, 0.375, 0.25, and 0.125, respectively). For small foil thicknesses, the propensity for populating $m = 0$ states is primarily driven by the shake-up process following the single-electron detachment of H^-. Remarkably, the propensity for populating $m = 0$ states extends to all foil thicknesses and, additionally, the population fractions are nearly independent of the foil thickness. This propensity is a consequence of the direction of the typical momentum transfers involved in the transport process: for high-velocity collisions, both elastic and inelastic momentum transfers are nearly perpendicular to the beam axis.

The propensity for populating $m = 0$ states is related to the fact that the direction of the momentum transfers gives rise to a propensity to create Stark states whose spatial probability densities have the largest polarization perpendicular to the beam axis. Within each Stark n-manifold, the most oriented states correspond the extreme $m = 0$ Stark states. The

population fractions of the various $|nkm\rangle$ Stark states within a given n-manifold obtained theoretically and experimentally [7] are in agreement with this picture. As an example, Fig. 3(b) shows the relative probability within the $n = 4$ $m = 0$ subshell for populating Stark states with *electric* quantum number $k = -3, -2, 2, 3$. Both experiment [7] and theory reveal population propensity of the extreme Stark states (large-k-states) $|4{-}30\rangle$ and $|430\rangle$ by about 50 % compared to the $|4{-}20\rangle$ and $|420\rangle$ states, in accordance with the dominance of transverse momentum transfers. As no external magnetic field is present during transport, the population of states with the same absolute *electric* quantum number should be equal. Small deviations from this rule are a measure of the statistical error of the calculations or the experimental uncertainties.

IV. QUANTUM TRANSPORT

Despite its apparent simplicity, a quantum calculation for the evolution of an electron described by the Hamiltonian in Eq. 2.1 is a formidable task in view of the large number of bound and continuum states that become populated for the momenta typically transferred to the electron. Thus far, the evolution of the electron in realistic ion-solid collisions has only been evaluated within the framework of classical dynamics. However, a fraction of the collisions suffered by the electron involve small momentum transfers for which excitation and ionization become classically suppressed [16]. We have recently undertaken the task of the developing a quantum transport scheme to address this problem [17, 18].

Formally, if $U(t_{n'}, t_n)$ denotes the evolution operator that evolves the state of the electron $|\Psi(t)\rangle\!\rangle$ from an instant of time t_n just before the n^th kick to an instant of time $t_{n'}$ just before the n^th kick (i. e. $|\Psi(t_{n'})\rangle\!\rangle = U(t_{n'}, t_n)|\Psi(t_n)\rangle\!\rangle$), then

$$U(t_n, t_0) = \prod_{k=0}^{n-1} U(t_{k+1}, t_k) \tag{4.1}$$

$$U(t_{k+1}, t_k) = e^{-i\,\mathcal{H}_{at}\,(t_{k+1}-t_k)}\;\; e^{i\,\vec{r}\cdot\Delta\vec{p}} \tag{4.2}$$

Thus, the calculation of the evolution of the electron is reduced to the evaluation of the

free evolution, $exp[-i\,\mathcal{H}_{at}\,(t_{k+1}-t_k)]$, and boost, $exp(i\,\vec{r}\cdot\,\Delta\vec{p})$, operators. An explicit matrix representation of Eq. 4.2 can be found by expanding the wavefunction in a complete orthonormal basis set composed of states $|n\rangle$,

$$|\Psi(t_{k+1})\rangle = \sum_{n,i,j} |n\rangle\ \langle n|e^{-i\,\mathcal{H}_{at}\,(t_{k+1}-t_k)}|i\rangle\ \langle i|e^{i\,\vec{r}\,\Delta\vec{p}}|j\rangle\ \langle j|\Psi(t_k)\rangle \tag{4.3}$$

In practice, only a finite basis set can be used. Since the evolution operator in Eq. 4.2 couples states of the complete Hilbert space, a finite dimensional representation of this operator is, in general, not unitary. In other words, if a finite basis set $\{|n\rangle\}$ is used, the norm of the wavefunction is not preserved. The amount of probability lost in this non-unitary calculation gives the probability flux to states outside the basis set. Matrix elements of the boost operator can be easily evaluated since they correspond to standard collisional form factors. In turn, an accurate non-unitary representation of the free evolution requires a more elaborate treatment such as the the complex dilatation method [19]. Because this approach neglects "back coupling" from states outside the basis into the finite basis set, the basis set must be large enough such that it becomes negligible (typically, convergence can be found using of the order of a thousand Sturmian pseudostates).

We have performed various tests in which the momenta transferred to the electron are kept constant but the time between kicks is randomly distributed. We have found that the amount of classically suppressed processes is reduced compared to the case of a single collision. This is due to the fact that some of these processes become classically allowed by the accumulation of energy and momentum transfers in multiple collisions. Work is underway to compare classical and quantum transport calculations for the full stripping process.

ACKNOWLEDGMENTS

Support for this work has been provided (a) by an ORNL Director's LDRD Program No. 3211-0846, (b) by the U.S. DOE, OBES, DCS, under Contract No. DE-AC05-96OR22464 with ORNL managed by LMER Corp. and (c) by the NSF.

REFERENCES

[1] *National Spallation Neutron Source Conceptual Design Report*, Oak Ridge National Laboratory Report NSNS/CDR-2 (1997), unpublished.

[2] *Outline Design of the European Spallation Neutron Source*, Edited by ISK Gardner, H. Lengeler, and G.H. Rees (1995), unpublished.

[3] B. Gervais, C. Reinhold, and J. Burgdörfer, Phys. Rev. A **53**, 3189 (1996).

[4] P. Kürpick, C. O. Reinhold, J. Burgdörfer, and B. Gervais, to be published in Phys. Rev. A.

[5] A. H. Mohagheghi et al Phys. Rev. A **43**, 1345 (1991).

[6] M.S. Gulley et al Phys. Rev. A **53**, 3201 (1996).

[7] P.B. Keating, et al to be published in Phys. Rev. A (1998).

[8] J. Burgdörfer, and J. Gibbons, Phys. Rev. **A 42** (1990) 1206.

[9] J.F. Hart and G. Herzberg, Phys. Rev. **106**, 79 (1957).

[10] J. C. Ashley, J. J. Cowan, R. H. Ritchie, V. E. Anderson, and J. Hoelzel, Thin Solid Films, **60**, 361 (1979).

[11] J. Neufeld and R. Ritchie, Phys. Rev., **98**, 1632 (1955); **99**, 1125 (1955).

[12] U. Fano, Annu. Rev. Nucl. Sci. **13**, 19 (1963).

[13] R. Abrines and I. C. Percival Proc. Phys. Soc. **88**, 861 (1966); **88**, 873 (1966); I. C. Percival and D. Richards Adv. At. Mol. Phys. **11**, 1 (1975).

[14] M. Born, *Vorlesungen Über Atommechanik*, (Springer, Berlin 1926); *The Mechanics of the Atom*, (G. Bell and Sons, London 1926)

[15] R. Becker and A. MacKellar, J. Phys. B, **17**, 39233 (1984); J. Pascale, C.O. Reinhold and R.E. Olson 1990 Phys. Rev. A **42**, 5305 (1990).

[16] C.O. Reinhold and J. Burgdörfer, J. Phys. B **26**, 3101, (1993).

[17] M. Melles, C. O. Reinhold and J. Burgdörfer, Nucl. Instr. Methods B**79**, 109, (1993); C. O. Reinhold, M. Melles, H. Shao, and J. Burgdörfer, J. Phys. B **26**, L659 (1993).

[18] S. Yoshida, C.O. Reinhold, J. Burgdörfer, B.E.Tannian, R.A.Popple and F.B.Dunning, to be published in Phys Rev A.

[19] A. Maquet, S. Chu, W.P. Reinhart, Phys. Rev. A **27**, 2946 (1983).

Figure captions

- Fig. 1: Total mean free path and mean free paths for elastic, inelastic longitudinal, and inelastic transverse collision as a function of beam energy in GeV.

- Fig. 2: Fraction of H^-, and $H(n = 1, 2, 3, 4)$ as a function of foil thickness for a beam energy of 0.8 GeV. The symbols correspond to the experimental data of Gulley et al [6].

- Fig. 3: Substate distributions in the $n = 4$-shell as a function of the foil thickness for a beam energy of 0.8GeV: (a) present calculations (lines) and experimental data of Keating et al. [7] (symbols) for the relative m-distribution. (b) present calculations (small symbols connected with lines) and experimental data of Keating et al. [7] (large for the population of the $m = 0$ Stark-states with *electric* quantum number $k = -3, -1, 1, 3$.

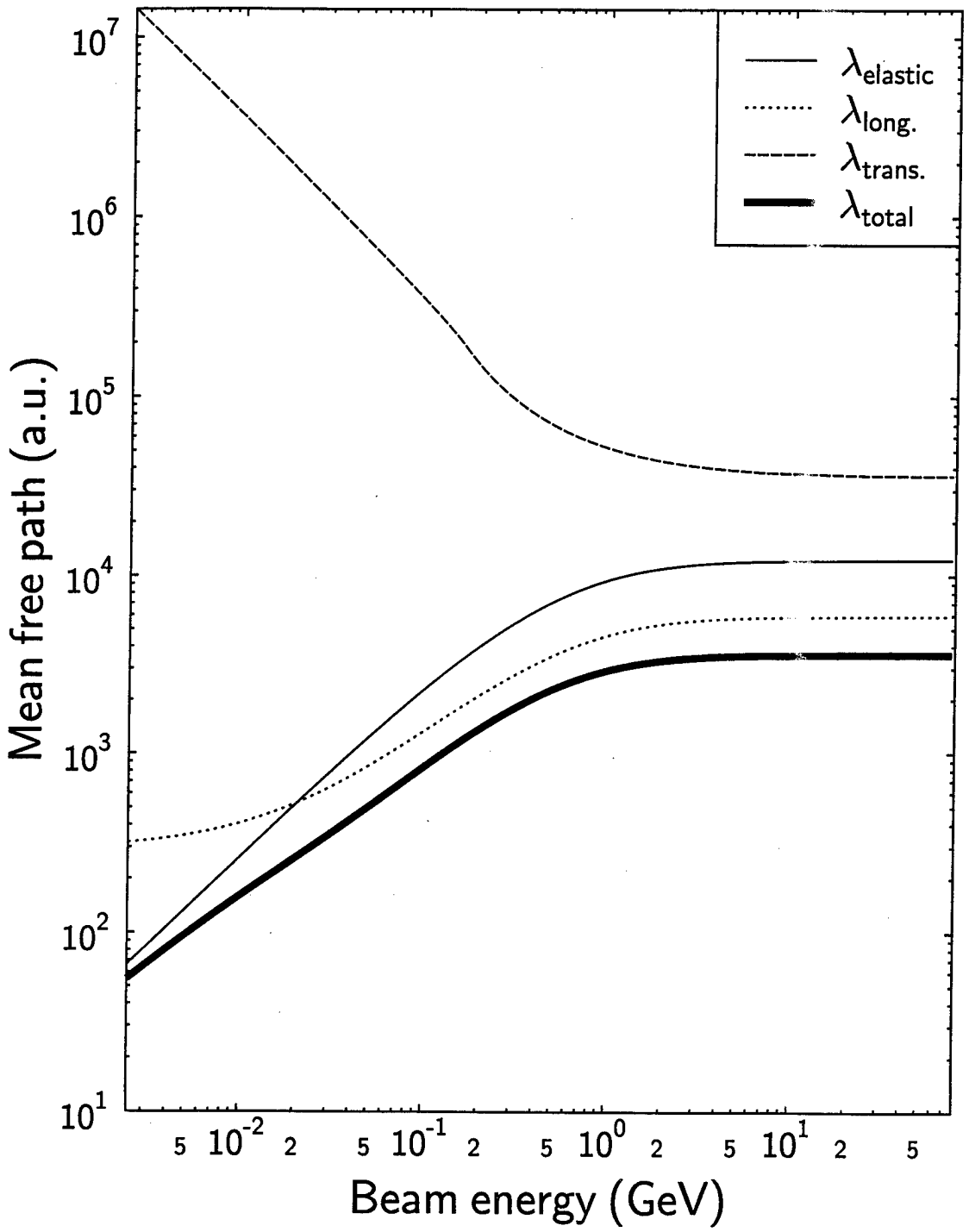
10^7
10^6
10^5
10^4
10^3
10^2
10^1
Mean free path (a.u.)
$\lambda_{elastic}$
$\lambda_{long.}$
$\lambda_{trans.}$
λ_{total}
5 10^{-2} 2 5 10^{-1} 2 5 10^{0} 2 5 10^{1} 2 5
Beam energy (GeV)

Fig. 1

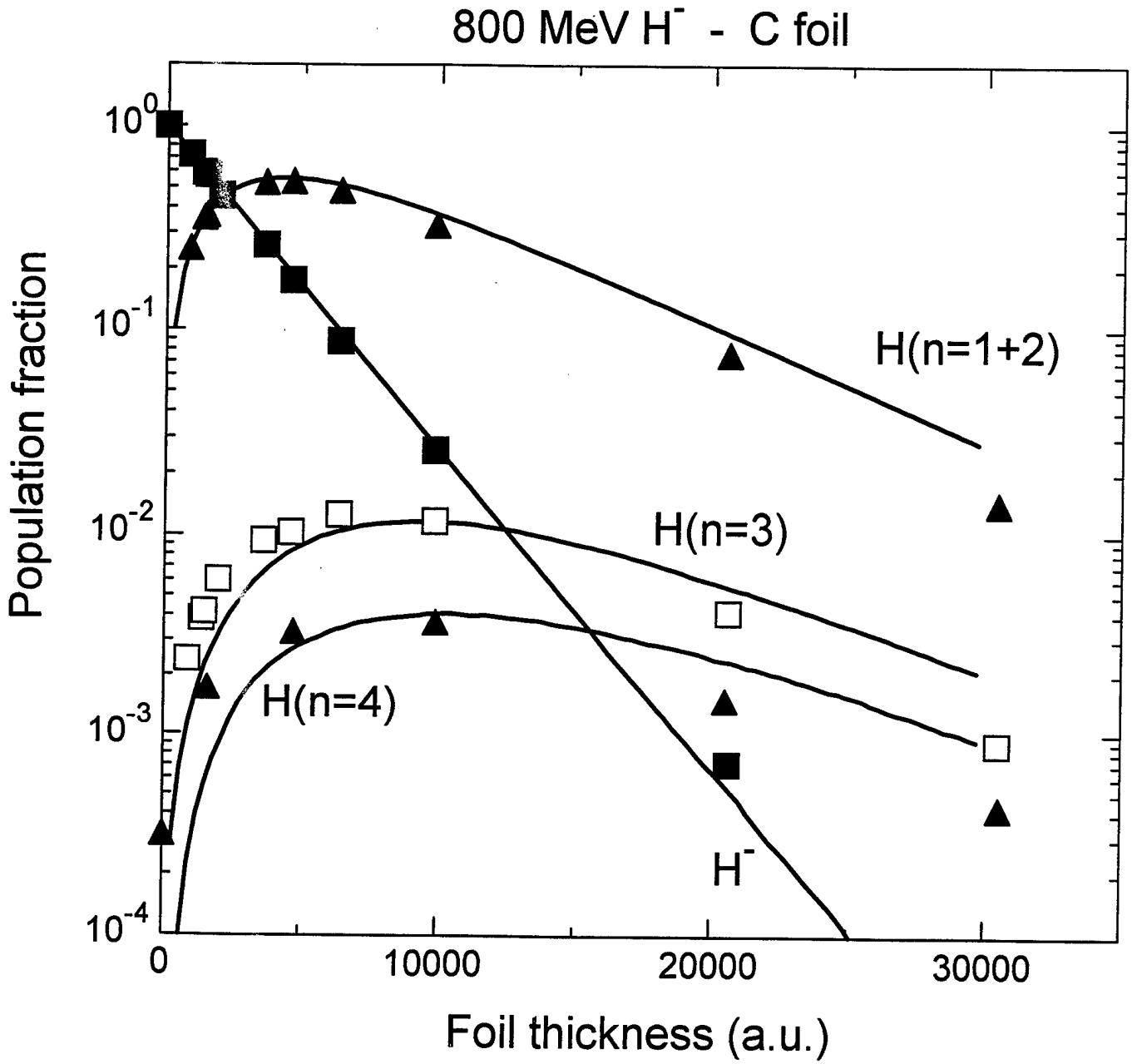
800 MeV H⁻ - C foil
Population fraction
10^0
10^-1
10^-2
10^-3
10^-4
H(n=1+2)
H(n=3)
H(n=4)
H⁻
0
10000
20000
30000
Foil thickness (a.u.)

Fig. 2

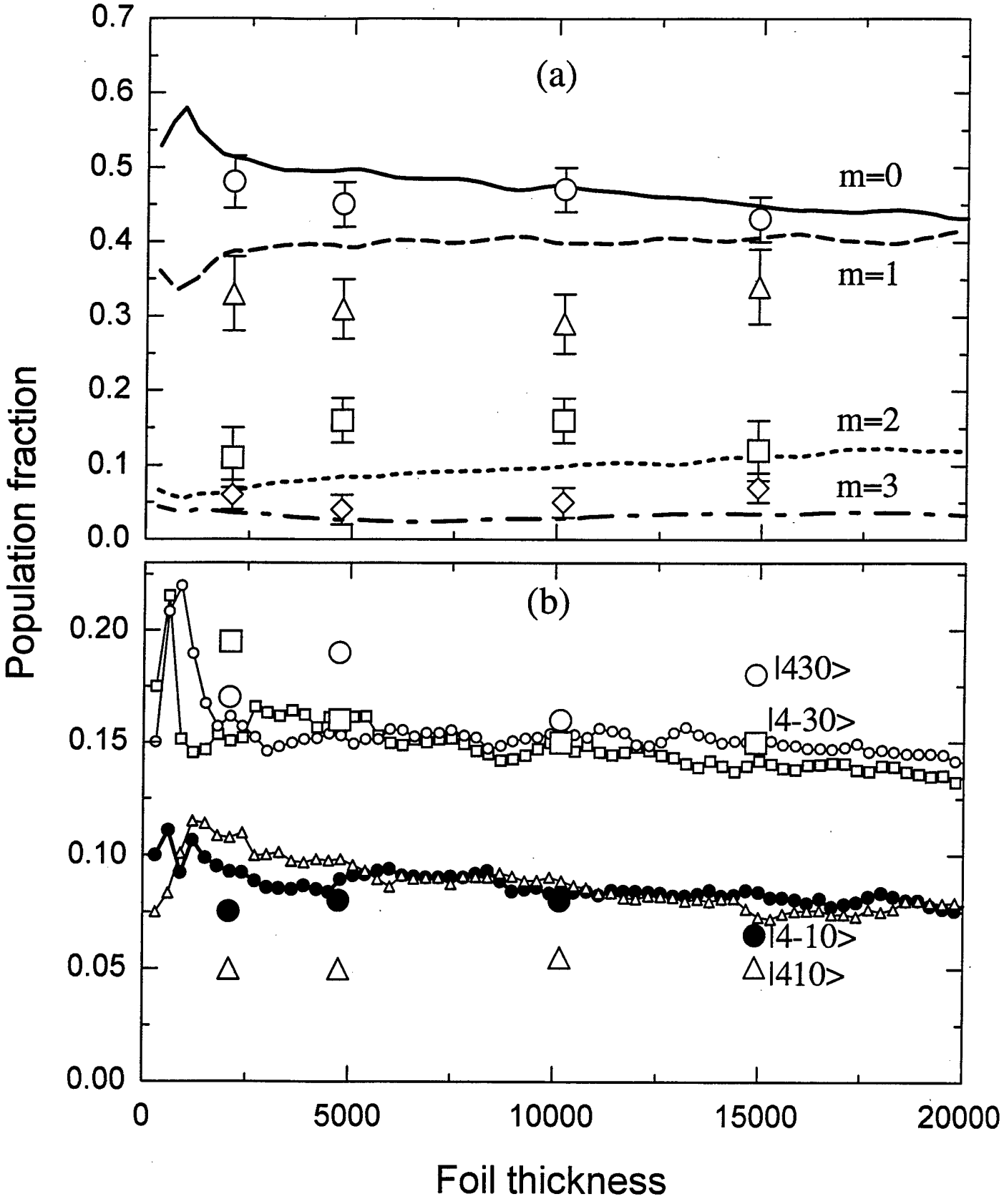
(a)
m=0
m=1
m=2
m=3
(b)
|430>
|4-30>
|4-10>
|410>
Population fraction
Foil thickness
0.7
0.6
0.5
0.4
0.3
0.2
0.1
0.0
0.20
0.15
0.10
0.05
0.00
0
5000
10000
15000
20000

Fig. 3

Report Number (14) ORNL/CP--98338
CONF-980564--

Publ. Date (11) 19980507
Sponsor Code (18) DOE/ER, XF
UC Category (19) UC-400, DOE/ER